Genomic analysis reveals a polygenic architecture of antler morphology in wild red deer (*Cervus elaphus*).

Lucy Peters[1*], Jisca Huisman[1], Loeske E.B. Kruuk[1,2],
Josephine M. Pemberton[1], Susan E. Johnston[1*]

[1]Institute of Evolutionary Biology, School of Biological Sciences, University of Edinburgh, Edinburgh, EH9 3FL, United Kingdom.
[2]Research School of Biology, The Australian National University, Canberra, Australia.
[*]Corresponding authors: Lucy.Peters@ed.ac.uk & Susan.Johnston@ed.ac.uk

Abstract

Sexually-selected traits show large variation and rapid evolution across the animal kingdom, yet genetic variation often persists within populations despite apparent directional selection. A key step in solving this long-standing paradox is to determine the genetic architecture of sexually-selected traits to understand evolutionary drivers and constraints at the genomic level. Antlers are a form of sexual weaponry in male red deer. On the island of Rum, Scotland, males with larger antlers have increased breeding success, yet there has been no response to selection observed at the genetic level. To better understand the underlying mechanisms of this observation, we investigate the genetic architecture of ten antler traits and their principle components using genomic data from >38,000 SNPs. We estimate the heritabilities and genetic correlations of the antler traits using a genomic relatedness approach. We then use genome-wide association and haplotype-based regional heritability to identify regions of the genome underlying antler morphology, and an Empirical Bayes approach to estimate the underlying distributions of

allele effect sizes. We show that antler morphology is heritable with a polygenic architecture, highly repeatable over an individual's lifetime, and that almost all aspects are positively genetically correlated with some loci identified as having pleiotropic effects. Our findings suggest that a large mutational target and pleiotropy with traits sharing similar complex polygenic architectures are likely to contribute to the maintenance of genetic variation in antler morphology in this population.

Introduction

Sexually-selected traits show a great variety and complexity across the animal kingdom, ranging from traits and behaviours that increase attractiveness, to those which increase intra-sexual competitiveness for access to mates (Andersson, 1994). Sexual traits are typically under strong selection (Kingsolver *et al.*, 2001), with phenotypic differences between related species suggesting that they can evolve rapidly, with downstream consequences for other phenomena such as adaptation, speciation and extinction probability (Lorch *et al.*, 2003; Ritchie, 2007; Servedio & Bürger, 2014; Wilkinson *et al.*, 2015; Martínez-Ruiz & Knell, 2017). Theory predicts that such strong sexual selection will reduce genetic variation within populations, yet empirical studies often show that sexual traits have substantial underlying genetic variation despite evidence of selection (Pomiankowski & Moller, 1995; Kotiaho *et al.*, 2001; Kruuk *et al.*, 2002; Svensson & Gosden, 2007). This contradiction presents an evolutionary paradox, for which several explanations have been proposed. These include differences in selection between the sexes, developmental stages or environmental conditions (Bourret *et al.*, 2017; Barson *et al.*, 2015), phenotypic plasticity (Charmantier & Gienapp, 2014), condition dependence (Dugand *et al.*, 2019) and trade-offs with survival (Johnston *et al.*, 2013). In addition, these observations could be due to genetic correlations with traits under opposing selection gradients and linkage disequilibrium between causal loci and deleterious alleles (Lande, 1982; Lande & Arnold, 1983; Connallon & Hall, 2018). Quantitative genetic studies have provided some insight into these different explanations, through estimating the relative contributions of additive genetic (i.e. the heritability, h^2) and environmental effects to phenotypic variance, as well as examining phenotypic and genetic correlations

with other traits, including fitness (Emlen, 1994; Griffith *et al.*, 1999; Kruuk *et al.*, 2002; Robinson *et al.*, 2006). However, a key limitation of most studies to date is that the genetic architecture of sexual traits is generally unknown - that is, the underlying loci, their number, distribution and relative effect sizes, and the extent of pleiotropy, epistatis and other interactions (Timpson *et al.*, 2018; Chenoweth & McGuigan, 2010). By identifying the genetic architecture of sexual traits, we can better understand the underlying molecular mechanisms and evolutionary processes that drive their variation (Dobzhansky, 1971; Lewontin *et al.*, 1974; Kuijper *et al.*, 2012; Wilkinson *et al.*, 2015).

Recent genomic advances in natural populations have led to a number of studies characterising genetic architectures using genome-wide association studies (GWAS, reviewed in Santure & Garant 2018). Yet, relatively few studies exist for sexually selected traits, with much of the focus on discrete traits with Mendelian or relatively simple genetic architectures (Johnston *et al.*, 2011; Barson *et al.*, 2015; Hendrickx *et al.*, 2021). In these rare cases, mapping specific genomic variants associated with sexual trait variation can allow investigation of sex, age and environment-specific effects at individual loci. As such, they have revealed compelling cases of heterozygote advantage due to trade-offs between reproductive success and survival (Johnston *et al.*, 2013), or due to differences in optimal trait expression between the sexes (Barson *et al.*, 2015). However in most cases, sexual traits are likely to have oligogenic or polygenic architectures (i.e. moderate to large numbers of underlying loci), particularly in cases where they are condition dependent (Rowe & Houle, 1996). One issue is that as the number of loci increase and their relative effect sizes decrease, it becomes more difficult to implicate individual loci in trait variation; for example, in heights of people of European ancestry, only a fraction of the loci underpinning variation has been identified (Yengo *et al.*, 2018). On the other hand, being able to determine that a trait has a polygenic architecture can still shed light on how sexual traits evolve for the following reasons. First, polygenic traits present a large mutational target, contributing to the maintenance of genetic variance via the introduction of new variants (Rowe & Houle, 1996). Second, selection induced allele frequency changes at a great number of loci is expected to result in a rapid change in trait mean, and thus trait evolution, which is sustained by the aforementioned large mutational input, leaving the distribution of genetic effects unperturbed (Barton *et al.*, 2017; Sella & Barton,

2019). Third, pleiotropy and/or linkage between loci could maintain variation through conflicts between traits sharing a similar or linked polygenic architecture (Ruzicka *et al.*, 2019). Therefore, studies of sexual traits should aim to identify specific genetic variants with large effects on phenotype, and should also aim also to determine the distribution of polygenic effect sizes and the degree to which these underlying loci are shared between traits. This will not only shed light on potential evolutionary processes and mechanisms in empirical studies, but will also inform the mechanistic details of theoretical models to allow better assumptions to account for the complexities of natural populations (McNamara & Houston, 2009; Wilkinson *et al.*, 2015).

Antlers are a form of sexual weaponry in deer (Cervidae) that are generally only present in males and are shed and regrown annually (Davis *et al.*, 2011). They are used as weaponry in intra-male competition for access to females, with larger antlers often associated with increased reproductive success (Kruuk *et al.*, 2002; Malo *et al.*, 2005), yet antler weights and dimensions are often moderately heritable in both wild and captive populations (Lukefahr & Jacobson, 1998; Williams *et al.*, 1994; Wang *et al.*, 1999; Van Den Berg & Garrick, 1997; Kruuk *et al.*, 2002, 2014; Jamieson *et al.*, 2020). In male red deer (*Cervus elaphus*) on the island of Rum, Scotland, there is directional selection for increased antler weight and number of points (known as “form”), yet both are substantially heritable (h^2 = 0.38 & 0.24, respectively) with no phenotypic response to selection observed over a 30 year study period (Kruuk *et al.*, 2002, 2014). Whilst both antler weight and form are positively genetically correlated, the selection gradients on the genetic components were estimated as zero and negative, respectively (Kruuk *et al.*, 2002, 2014). This suggested that selection for antler weight is environmentally driven, whereas negative selection on antler form is constrained by genetic associations with a trait that is genetically unresponsive to selection, meaning that genetic constraints may contribute to the maintenance of genetic variance. Alternatively, the association with breeding success may be driven by indirect correlations with environmental variables (Kruuk *et al.*, 2014). To better understand the mechanisms constraining selection, a logical next step is to determine the genetic architecture of antler morphology. As antlers present a multi-dimensional phenotype, adding more information from different measures may contribute to understanding potential evolutionary conflict and constraints within the antler

and to characterise the specific genetic variants underpinning heritable variation (Chenoweth & McGuigan, 2010).

In this study, we used an extensive antler morphology data set with 948 to 3972 observations in 336 to 891 unique males and genomic data from 38,000 polymorphic SNPs to estimate the heritability and genetic correlations of ten antler traits using genomic relatedness matrices. We then use genome-wide association and haplotype-based regional heritability to identify regions of the genome underlying antler morphology, and an Empirical Bayes approach to estimate the underlying distributions of allele effect sizes. We show that antler morphology is heritable with a polygenic architecture, and that almost all aspects are positively genetically correlated with some loci identified as having pleiotropic effects. Our findings suggest that genetic variation in antler morphology is maintained via a large mutational target and pleiotropy with traits sharing similar complex polygenic architectures in the red deer population.

Methods

Study system

The red deer study population is situated in the North Block of the Isle of Rum, Scotland (57°02'N, 6°20'W) and has been subject to individual monitoring since 1971 (Clutton-Brock *et al.*, 1982). Deer calves are marked with ear tags shortly after birth to enable recording of detailed life histories of individuals. DNA is routinely extracted from neonatal ear punches, post-mortem tissue and/or cast antlers (see Huisman *et al.* 2016). A pedigree of 4,515 individuals is available for the population, and was previously constructed using single nucleotide polymorphism (SNP) data in the R package Sequoia (Huisman, 2017). Research was conducted following approval of the University of Edinburgh's Animal Welfare and Ethical Review Body and under appropriate UK Home Office licenses.

Antler measures

Male red deer cast and regrow their antlers every year from the age of one or two (Kruuk *et al.*, 2002). Ten antler measures are routinely taken from cast antlers and antlers from deceased individuals between 1971 and 2017 (see Figure 1 and Table 1 for full details and sample sizes of each measure). All measures of length were taken following the curve of the antler, and measures of circumference were taken at the narrowest point between antler tines (points). Total antler length was defined as the distance from the coronet (base) to the furthest point of the antler. All length and circumference measures were taken in centimetres. Antler weight was measured as the total dry mass of the antler in grams. Antler form was defined as the number of tines, and as this trait can be determined visually on living deer, was determined from observations in the field and therefore has the greatest sample size (3972 observations from 891 stags). Where measurements from both the left and right antlers were available, the mean was taken. Individual measurements were excluded if the antler part was broken and antler weight was discarded if any part of the antler was broken. Only antlers from stags aged 3 years or older were considered, as cast

antlers recovered in the field can be reliably assigned to known individuals by their shape from this age onwards (Kruuk *et al.*, 2002, 2014).

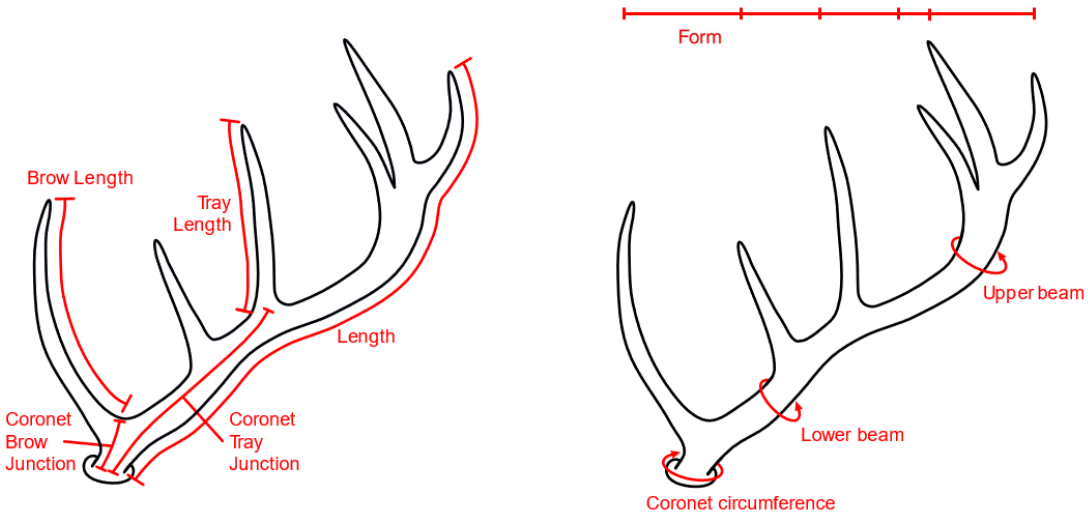

Figure 1: A schematic of the antler measures used in this study (measured in *cm*). Antler weight was also measured in *g*. Further details for each measurement are given in the main text and in Table 1.

Table 1: Summary statistics of all 10 antler measures as shown in Figure 1 in SNP genotyped males. *N Obs* is the number of observations, *N IDs* is the number of unique individuals for each measure. All lengths and circumferences were measured in *cm*, weight was measured in *g*. *SD* denotes the standard deviation.

Trait	N Obs	N IDs	Mean	SD
Antler Length	1060	444	65.168	12.029
Coronet Circumference	1224	471	15.626	2.013
Lower Beam Circumference	1204	460	10.504	1.533
Upper Beam Circumference	1123	436	9.446	1.358
Coronet-Brow Junction	1162	466	5.720	1.025
Coronet-Tray Junction	1184	455	27.313	5.398
Brow Length	1139	457	20.568	5.461
Tray Length	948	388	14.484	4.177
Antler Weight	1003	336	649.858	243.098
Form (Total Number of Points)	3972	891	4.498	1.072

Genomic data-set

DNA samples from 2,870 individuals have been genotyped at 51,248 SNP markers (Huisman *et al.*, 2016) on the Cervine Illumina BeadChip (Brauning *et al.*, 2015) using an Illumina genotyping platform and Illumina GenomeStudio software (Illumina Inc., San Diego, CA, USA). All SNPs on the Cervine Illumina BeadChip are named based on their synteny with the cattle genome BTA vUMD 3.0 (e.g. SNP ID *cela1_red_15_1479373* is orthologous to position 1479373 on cattle chromosome 15). In addition, a linkage map specific to the Rum population is available, with 38,083 SNPs assigned to linkage groups corresponding to the 33 deer autosomes and X chromosome (Johnston *et al.*, 2017). Quality control was carried out in PLINK v1.9 (Chang *et al.*, 2015) with the following thresholds: SNP genotyping success >0.99, minor allele frequency >0.01 and individual genotyping success >0.99. Further quality control of mapped SNPs and X-linked markers (i.e heterozygous state in males) was conducted using the *check.marker* function with

default thresholds in the R library GenABEL v1.80 in R v3.4.2 (Aulchenko *et al.*, 2007). The final SNP dataset consisted of 2,138 individuals and 38,006 markers. Genome-wide linkage disequilibrium (LD) was calculated between all SNPs within 1Mb of each other using Spearman's Rank correlation (ρ). Based on a linear regression of ρ on the log base pair distance between SNPs, LD decayed at a relatively low rate of 0.031 ρ per Mb (SE = 5.56×10^{-4}, Figure S1).

Principal components of antler measures

A principal component analysis (PCA) was conducted to create a second dataset combining information from the different antler measures, while also increasing the differentiation among the different principal components (PCs). As PCA does not allow for missing data, we imputed missing antler measures using the Bayesian *bpca* algorithm in the packages pcaMethods v1.7 in R v3.4.2 (Stacklies & Redestig, 2018; Oba *et al.*, 2003). We used the default settings which assumes a flat prior distribution for imputation, and the most appropriate number of PCs was determined using the *kEstimate* function. To improve imputation accuracy, the form was split into the number of tines on the lower beam and upper beam, respectively, resulting in 11 antler measures. Imputation accuracy was quantified by calculating the error of prediction (E) from a complete subset of the data with no missing values and the same subset with randomly missing data at a similar level to the whole data set ($\sim$ 9%). The error of prediction was calculated as follows:

$$E = \sum (V - I)^2 / \sum (V)^2 \tag{1}$$

where I refers to the imputed values of the data subset with missing values and V to their counterpart in the complete data subset (Stacklies & Redestig, 2018). Our analysis fount that the imputation of missing values using a Bayesian PCA approach achieved high accuracy (E = 0.015). To account for variation among antlers due to age structure, antler measure values were modelled using a linear model approach (following Pallares *et al.* 2014). All models had the same structure:

$$y = Age + Age^2 + e \tag{2}$$

where y is a vector of the antler measure and e is a residual error term. Age effects were fitted as a fixed quadratic term to account for the non-linear change in antler measures with age (see also Nussey *et al.* 2009 and Kruuk *et al.* 2002). All antler measures were modelled using a Gaussian distribution. All models were fitted using the *lm* function in R v3.4.2. The residuals of these models were then used in a standard PCA using the *prcomp* function in R and the scores of the PCs used as trait values in the downstream analysis.

Estimating heritability using the animal model

All antler measures and PCs were modelled using a restricted maximum-likelihood (REML) approach within the mixed 'animal model' framework (Henderson, 1975) in ASREML-R v4.0 (Butler *et al.*, 2009) in R v3.4.2. The animal model estimates the effect sizes of fixed effects and partitions phenotypic variance (V_P) into several random effects, including the variance attributed to additive genetic effects (V_A). Previous studies have estimated V_A using a pedigree relatedness matrix (Kruuk *et al.*, 2002, 2014); here, we wished to compare estimates of V_A using both pedigree and genomic relatedness information. Therefore, all models were carried out estimating V_A in one of two ways: 1) using a numerator relationship matrix A based on the pedigree, using the *ainv* function in ASReml-R; and 2) using a genomic relatedness matrix (GRM) calculated using autosomal SNPs (N = 37,271) in the *--make-grm function* in GCTA v1.24.3 (Yang *et al.*, 2011a). The GRM was adjusted to assume similar frequency spectra of genotyped and causal loci with the argument *--grm-adj 0*.

All 10 antler measures and 11 PCs were modelled in univariate animal models with the following structure:

$$y = X\beta + Z_1 a + Z_r u_r + e \quad (3)$$

where y is a vector of the antler measure or PC, X is an incidence matrix relating individual measures to the vector of fixed effects β; Z_1 and Z_r are an incidence matrices relating individual measures to additive genetic and other random effects respectively; a is a vector of relatedness matrix A or GRM; u_r is a vector of additional random effects; and e is a vector of residual effects. Fixed effects included age in years as a both a linear and

quadratic term for the antler measures and an intercept only for the PC models (as age structure was accounted for prior to PC estimation). Random effects included: the additive genetic effect; permanent environment (i.e. individual identity) to account for pseudoreplication due to repeated measures in the same individual; and birth year and year of antler growth to account for common environmental effects between individuals. The narrow sense heritability (h^2) was calculated as V_A/V_P, where V_P was defined as the sum of the variance attributed to all random effects, including the residual variance (Falconer & Mackay, 1996). The significance of fixed effects was calculated with a Wald test, while the significance of the random effects was tested using a likelihood ratio test (LRT) between models with and without random effect of interest (i.e. 2 $\times$ the difference between the model log-likelihoods, assuming a χ^2 distribution with 1 degree of freedom).

Bivariate models were run to determine genetic correlations between the 10 antler measures, with the following structure:

$$\begin{bmatrix} y_1 \\ y_2 \end{bmatrix} = \begin{bmatrix} X_1 & 0 \\ 0 & X_2 \end{bmatrix} \begin{bmatrix} \beta_1 \\ \beta_2 \end{bmatrix} + \begin{bmatrix} Z_1 & 0 \\ 0 & Z_2 \end{bmatrix} \begin{bmatrix} a_{a1} \\ a_{a2} \end{bmatrix} + \begin{bmatrix} Z_{r1} & 0 \\ 0 & Z_{r2} \end{bmatrix} \begin{bmatrix} u_{r1} \\ u_{r2} \end{bmatrix} + \begin{bmatrix} e_1 \\ e_2 \end{bmatrix} \quad (4)$$

All variables are as defined in equation (3), with subscripts referring to antler traits 1 and 2, respectively. The GRM was used to model the additive genetic covariance. The genetic correlation r^2 can be obtained from the genetic covariance, as $r_a = cov_a(1,2)/\sigma_1\sigma_2$, where $cov_a(1,2)$ stands for the covariance between trait 1 and 2, and σ represents the respective standard deviations for traits 1 and 2. The significance of r_a was determined using an LRT as above, by comparing the model to another where r_a was constrained to either zero or one.

Genome-wide association studies

Genome-wide association studies (GWAS) were conducted in RepeatABEL v1.1 (Rönnegård *et al.*, 2016) implemented in R v3.4.2. First, the *prefitModel* function was used to fit a linear mixed model (without fixed SNP effects), specifying the same fixed and random effect structure as Equation 3. The resulting covariance matrix of the random

effects was then input to the *rGLS* function, which fits each SNP genotype as an additive linear covariate. This approach accounts for population structure by fitting the GRM as a random effect and allows for repeated measures per individual. The significance of each SNP was determining using Wald tests, distributed as χ^2 with 1 degree of freedom. These statistics were corrected for potential inflation due to population structure not captured by the GRM by dividing them by the genomic inflation factor λ, defined as the observed median χ^2 statistic divided by the null expectation median χ^2 statistic (Devlin & Roeder, 1999). This was done separately for each antler measure. After correction, the genome-wide significance threshold was set to a p-value of 1.42×10^{-6}, equivalent to α= 0.05 after correcting for multiple-testing and accounting for non-independence due to LD between SNP markers (see Johnston *et al.* 2018).

Regional heritability analysis

In addition to GWAS, we used a regional heritability approach to identify regions of the genome associated with antler trait variation. This method uses information from multiple loci to determine the proportion of V_P explained by defined genomic regions, and has increased power to detect variants of small effect sizes and low minor allele frequencies (Yang *et al.*, 2011b; Nagamine *et al.*, 2012). Regions were defined using a 'sliding window' approach with SNPs of known position on the Rum deer linkage map (Johnston *et al.*, 2017). Each window was 20 SNPs wide and overlapped the preceding window by 10 SNPs. If the last window in the linkage group contained less than 20 SNPs, the last 20 SNPs of that linkage group were taken instead. SNPs in linkage group 34, which corresponding to the X chromosome, were excluded from this analysis, as models using X-linked markers did not converge. This resulted in a total of 3,608 genomic windows. The contribution of each genomic region to V_A and V_P for each antler measure and PC was modelled as follows:

$$y = X\beta + Z_1(a - v_i) + Z_2 v_i + Z_r u_r + e \tag{5}$$

with variables defined as in Equation (3), but with the additive genetic components split into two terms: $Z_1(a - v_i)$ and $Z_2 v_i$, where Z_1 is an incidence matrix of the GRM

constructed based on all autosomal SNPs excluding those in window i, $(a - v_i)$ is the additive genetic effect excluding the window i; Z_2 is an incidence matrix of the GRM constructed with only the SNPs in window i and v_i is the additive genetic effect of the window i. The significance of an association between a window i and an antler trait was determined using a LRT comparing models containing and omitting the term $Z_2 v_i$. The distribution of χ^2 statistics from the LRTs across all windows was corrected using the genomic control parameter λ, calculated using the same approach as above (Devlin & Roeder, 1999). A genome-wide significance threshold was calculated using a Bonferroni correction, where the α significance level (here 0.05) was divided by the number of effective tests. For this, we divided the number of windows by two to account for the overlap of half the number of total SNPs within each window, resulting in a significance threshold of P = 2.77×10^{-5}.

Estimation of SNP effect size distribution

We investigated the distribution of allele effect sizes and false discovery rates for all antler measures and PCs using the *ash* function in the R package ashR v2.2-32 (Stephens, 2016). This uses "adaptive shrinkage", an Empirical Bayes method that uses the slopes and standard errors of the additive SNP effects from the GWAS models above to compute a posterior distribution of SNP effect sizes across all loci. This approach estimates the local false discovery rate (*lfdr*), which is the probability that the SNP effect is zero. The significance of a SNP effect was then determined by a local false sign rate (*lfsr*), defined as the probability of making an error when assigning a sign (positive or negative) to an effect, with a cut-off at α = 0.05. The prior distribution was specified to be any symmetric unimodal distribution when applying the *lfdr* estimation.

We then re-estimated the effect sizes of SNPs with the highest non-zero effects using adaptive shrinkage using the animal model framework (Equation 3) in ASREML-R v4.0 (Butler *et al.*, 2009). A maximum number of 10 SNPs per trait were taken. SNP genotype was fit as a two or three level factor and significance was tested using a Wald test. Fitting SNP genotype as a factor allowed the quantification of both the dominance deviation and

the variance co-variance structure of the genotypes, which are needed to estimate the variance attributed to each SNP, calculated as follows (Falconer & Mackay, 1996):

$$V_{SNP} = 2pq(a + d(q - p))^2 \quad (6)$$

where p and q are the allele frequencies of alleles A and B, respectively; a is the additive genetic effect defined as the mid-point between the effect sizes of the genotypes AA and BB; and d is the dominance deviation defined as the difference between a and the effect size of the heterozygote AB. The proportion of V_A attributed to a SNP was calculated as the ratio of V_{SNP} to the sum of V_{SNP} and the V_A obtained from an animal model where the SNP effect was omitted. Standard errors of V_{SNP} were estimated using the *deltamethod* function in the R library msm v1.6.7 (Jackson, 2011) in R v3.4.2.

Data Accessibility Statement

Data for this study will be archived in a public repository upon manuscript acceptance. All results and data underlying the figures in this manuscript are provided as Supplementary Material. All scripts for the analysis are provided at https://github.com/Lucy-Peters/Red_deer_antler_genetic_architecture.

Results

Principal component analysis of antler measures

A principal component analysis (PCA) of 11 antler measures resulted in the maximum number of principal components (i.e. 11 PCs). The composition of the PCs showed that PC1, which explained around 41% of the variance, combined approximately equal amounts of information from all 11 measures, while PCs 2 to 11 explained increasingly less variance, mostly representing one or two antler measures (Figure 2).

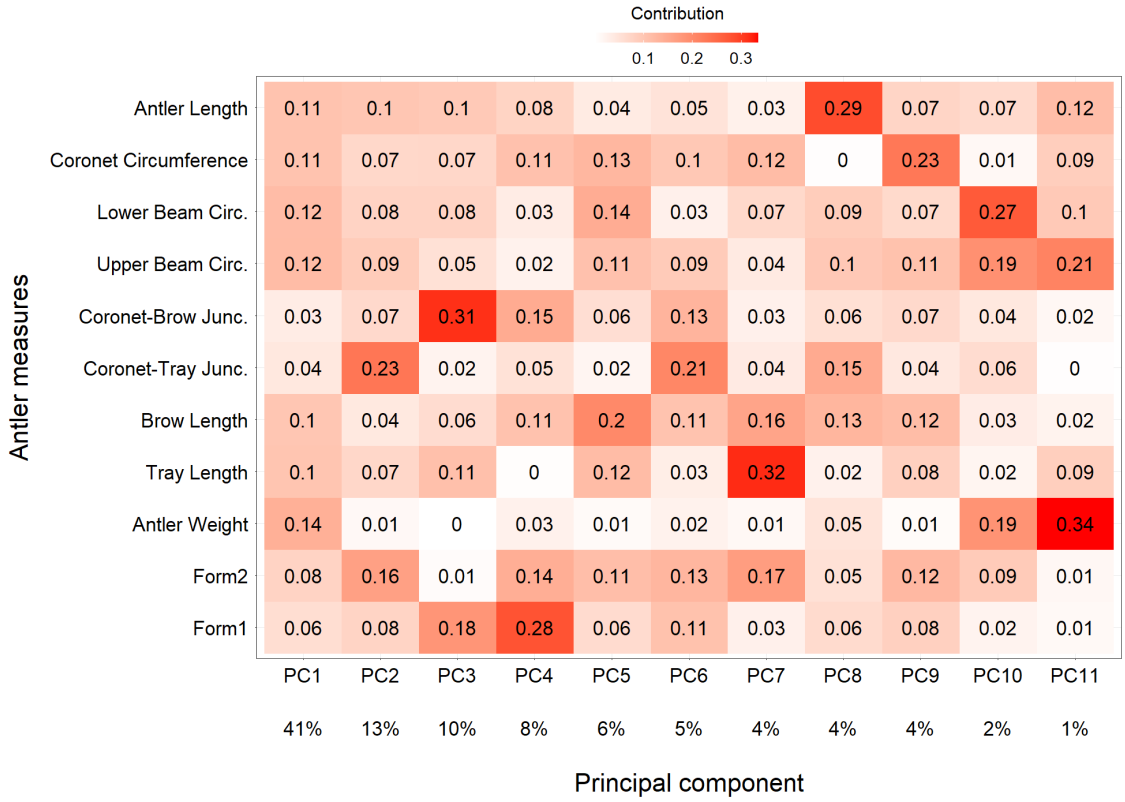

Figure 2: Heat-map showing the contribution (as a proportion) of each antler measurement to each of the 11 principal components.

Animal models of antler measures.

Antler measures were significantly heritable, with estimates ranging from h^2 = 0.211 to 0.436 for the pedigree estimates, and h^2 = 0.229 to 0.414 for the genomic estimates (Figure 3; Tables 2 & S1). Heritability estimates for antler weight, antler length, coronet circumference, brow length and form were generally consistent with previous findings by Kruuk *et al.* (2014, Figure 3). All antler PCs were also significantly heritable, although estimates decreased substantially for higher order PCs, which explained relatively small proportions of variance in antler morphology (Figure S2, Table S2). For all antler measures and PCs, confidence intervals between pedigree and genomic relatedness estimates were highly similar; there was no trend when comparing estimates of h^2 for the same trait, suggesting that both the pedigree and genomic relatedness matrices capture the additive genetic variance to a similar degree in this population. Therefore, all results described from this point onwards are from models fitting a GRM, unless otherwise stated.

The permanent environmental effect (which includes dominance and epistatic effects) was generally significant for all antler measures, explaining up to 28.0% (upper beam circumference) of the phenotypic variance (Table 2). Year of antler growth explained a significant proportion of phenotypic variance for most antler measures and PCs (Tables 2 and S2, respectively). Conversely, birth year was not significant for any antler measure or PC; nevertheless, we retained this random effect in all models to account for potential cohort effects (Tables 2 & S2). Trait repeatabilities, calculated as the sum of contributions from the additive genetic, the permanent environment and birth year components, was high for all antler measures, ranging from 38.5% (antler length) to 66.1% (tray length; Table 2). Age as both linear and quadratic fixed effect terms was significantly associated with all antler measures (Table S3).

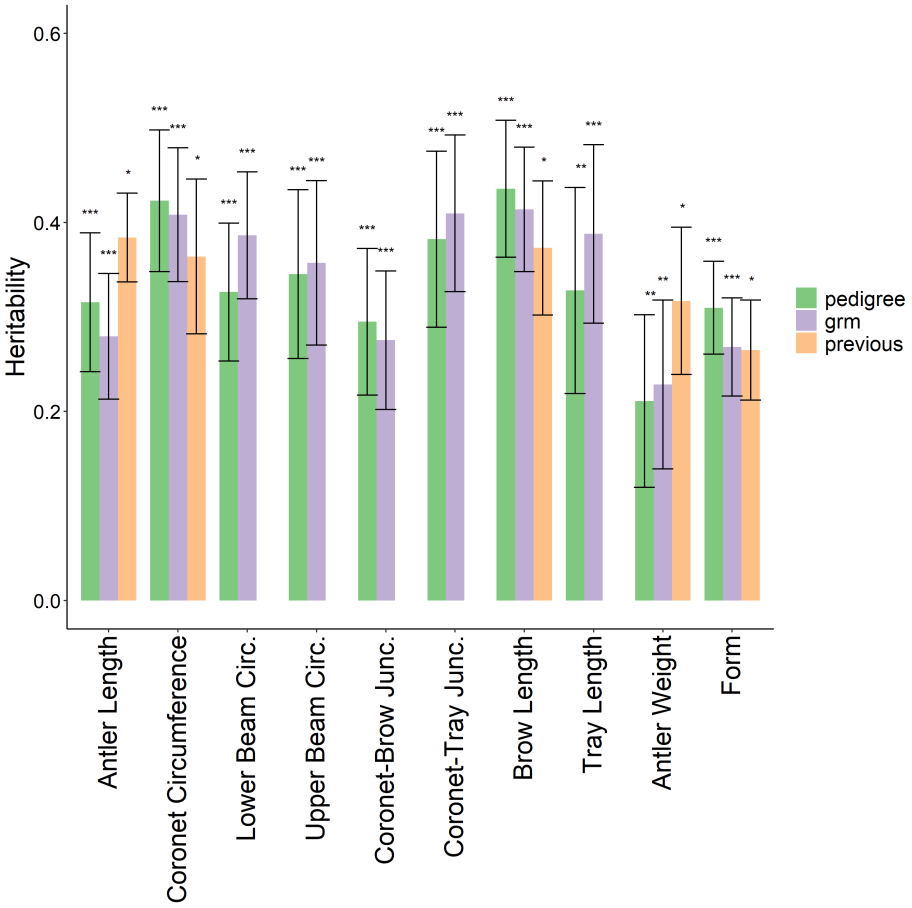

Figure 3: Heritability estimates for all 10 antler measures. Both estimates from the pedigree and the GRM models are shown as well as results from a previous study by Kruuk *et al.* (2014) for antler weight and form. $^{*}P \leq 0.05$, $^{**}P \leq 0.01$ and $^{***}P \leq 0.001$. Underlying data is provided in Table S1

Table 2: Proportions of phenotypic variance (V_P) explained by random effects in animal models of the ten antler measures. The additive genetic effect was estimated using the GRM. Standard errors are given in brackets. Information on sample sizes and mean measures is provided in Table 1.

Trait	V_P	Additive Genetic	Permanent Environment	Birth Year	Growth Year	Residual	Repeatability
Antler Length	61.155	0.279 (0.066)	0.105 (0.058)	1.04E-08 (0.014)	0.222 (0.047)	0.393 (0.035)	0.385
Coronet Circ.	3.047	0.408 (0.071)	0.128 (0.056)	0.018 (0.018)	0.243 (0.047)	0.203 (0.020)	0.554
Lower Beam Circ.	1.323	0.386 (0.067)	0.096 (0.054)	2.22E-07 (1.64E-08)	0.211 (0.042)	0.307 (0.027)	0.483
Upper Beam Circ.	1.084	0.357 (0.087)	0.280 (0.081)	5.16E-08 (0.017)	0.164 (0.035)	0.199 (0.018)	0.637
Coronet-Brow Junc.	0.872	0.275 (0.073)	0.254 (0.068)	0.026 (0.022)	0.152 (0.037)	0.292 (0.025)	0.555
Coronet-Tray Junc.	20.930	0.410 (0.083)	0.148 (0.072)	0.001 (0.016)	0.019 (0.009)	0.422 (0.032)	0.559
Brow Length	21.555	0.414 (0.066)	0.068 (0.050)	6.33E-09 (0.013)	0.269 (0.050)	0.250 (0.025)	0.481
Tray Length	13.809	0.388 (0.094)	0.273 (0.088)	7.65E-08 (5.34E-09)	0.028 (0.012)	0.311 (0.028)	0.661
Antler Weight	30727.710	0.229 (0.089)	0.263 (0.086)	0.023 (0.027)	0.252 (0.050)	0.233 (0.025)	0.514
Form	0.907	0.268 (0.052)	0.249 (0.046)	0.024 (0.015)	0.044 (0.011)	0.416 (0.019)	0.541

Genetic correlations between antler measures

Most antler measures were positively genetically correlated, suggesting some degree of shared genetic architecture (Table 3). This was also reflected in the disproportionate contribution of all antler measures to PC1 (Figure 2). Antler weight was significantly positively correlated with almost all other measures (with the exception of coronet-tray junction), ranging from r^2 = 0.40 for coronet-brow junction to r^2 = 0.94 for upper beam circumference. The only significant negative genetic correlations were observed between coronet-tray junction and tray length, form and lower beam circumference (Table 3).

Genome-wide and regional heritability studies

No genomic regions were significantly associated with any antler measure or PC using GWAS (Figures 4 and S3, and Tables S4 and S5, respectively). The regional heritability analysis found no regions of the genome significantly associated with any antler measure or PC (Figures 5 and S4, and tables S6 and S7, respectively), with the exception of PC9, which was significantly associated with three overlapping windows (corresponding to a $\sim$4.4 Mb region) on CEL linkage group 21. The most significantly associated window explained 16.8% (SE = 8.0%) of the phenotypic variance and 66.3% (SE = 22.0%) of the additive genetic variance. However, PC9 accounts for only 4% of overall phenotypic variance among all antler measures (see Figure 2). Homology with the cattle genome (version ARS-UCD1.2) suggested that there are a total of 19 coding regions within the region covered by all three significant windows, Details of SNPs within this region can be found in Table S8 and associated GO terms can be found in Table S9.

Table 3: Genetic correlations among all 10 antler measurements. Standard errors are given in brackets, *$P \leq 0.05$, **$P \leq 0.01$ and ***$P \leq 0.001$. AL = Antler Length, CC = Coronet Circumference, LBC = Lower Beam Circumference, UBC = Upper Beam Circumference, CBJ = Coronet-Beam Junction, CTJ = Coronet-Tray Junction, BL = Brow Length, TL = Tray Length, AW = Antler Weight, F = Form.

	CC	LBC	UBC	CBJ	CTJ	BL	TL	AW	F
AL	0.678 (0.068) ***	0.640 (0.077) ***	0.664 (0.093) ***	0.674 (0.103) ***	0.665 (0.096) ***	0.549 (0.075) ***	0.447 (0.109) ***	0.854 (0.063) ***	0.406 (0.108) ***
CC	—	0.800 (0.054) ***	0.745 (0.084) ***	0.168 (0.109)	0.369 (0.089) ***	0.650 (0.067) ***	0.603 (0.088) ***	0.913 (0.065) ***	0.565 (0.095) ***
LBC	—	—	0.940 (0.024) ***	0.442 (0.102) ***	-0.322 (0.091) ***	0.592 (0.068) ***	0.810 (0.059) ***	0.928 (0.059) ***	0.780 (0.064) ***
UBC	—	—		0.266 (0.132) *	-0.179 (0.112)	0.541 (0.073) ***	0.733 (0.069) ***	0.943 (0.059) ***	0.902 (0.041) ***
CBJ	—	—	—	—	0.492 (0.108) ***	-0.079 (0.109)	-0.006 (0.137)	0.396 (0.185) *	-0.163 (0.126)
CTJ	—	—	—	—	—	0.055 (0.065)	-0.713 (0.073) ***	0.188 (0.146)	-0.521 (0.099) ***
BL	—	—	—	—	—	—	0.739 (0.070) ***	0.710 (0.073) ***	0.608 (0.065) ***
TL	—	—	—	—	—	—	—	0.811 (0.082) ***	0.822 (0.064) ***
AW	—	—	—	—	—	—	—	—	0.890 (0.061) ***

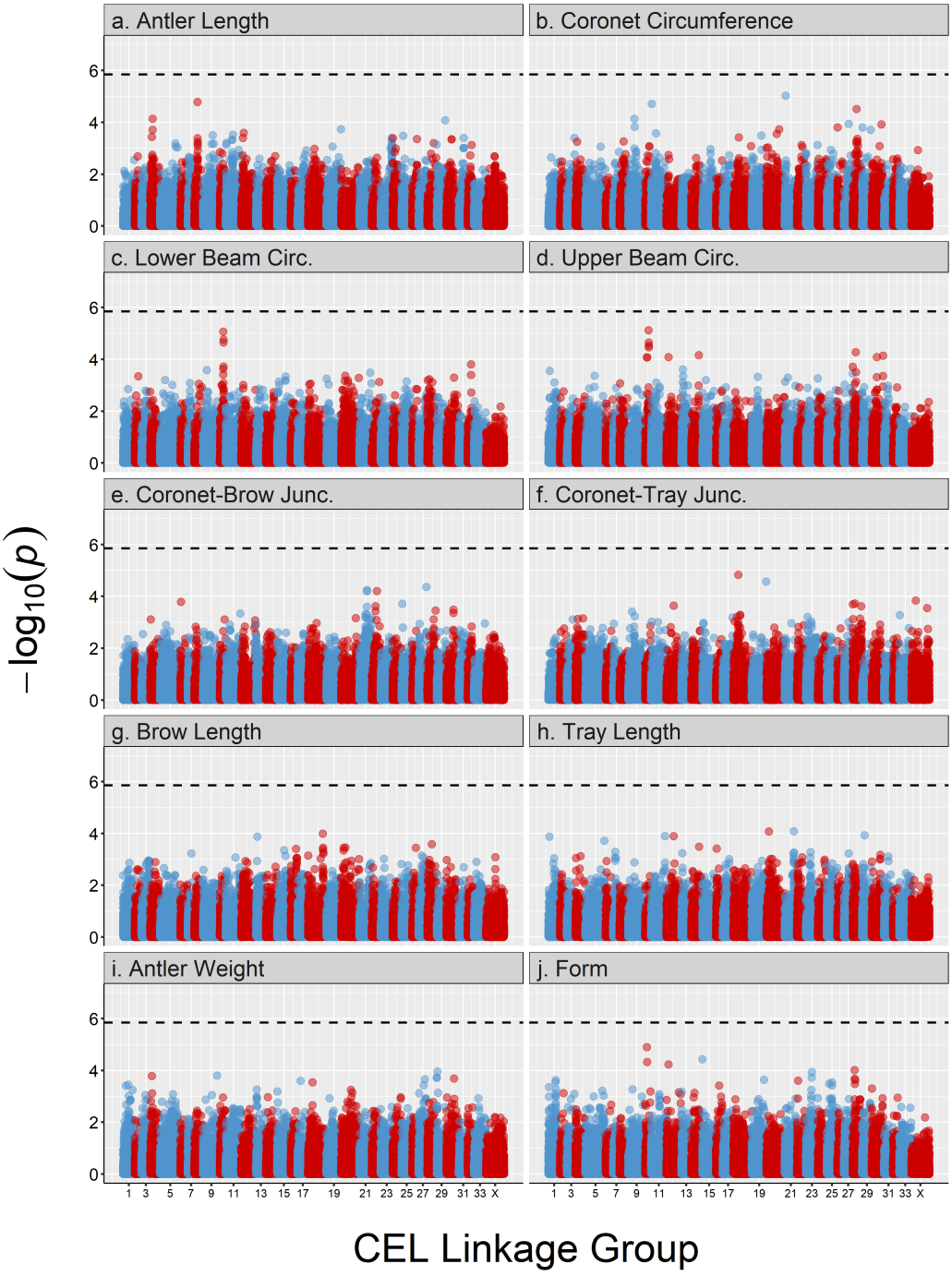

Figure 4: Genome-wide association study for antler measures. The dashed line indicates the significance threshold equivalent to α = 0.05. Points are colour-coded by chromosome. Underlying data is provided in Table S4.

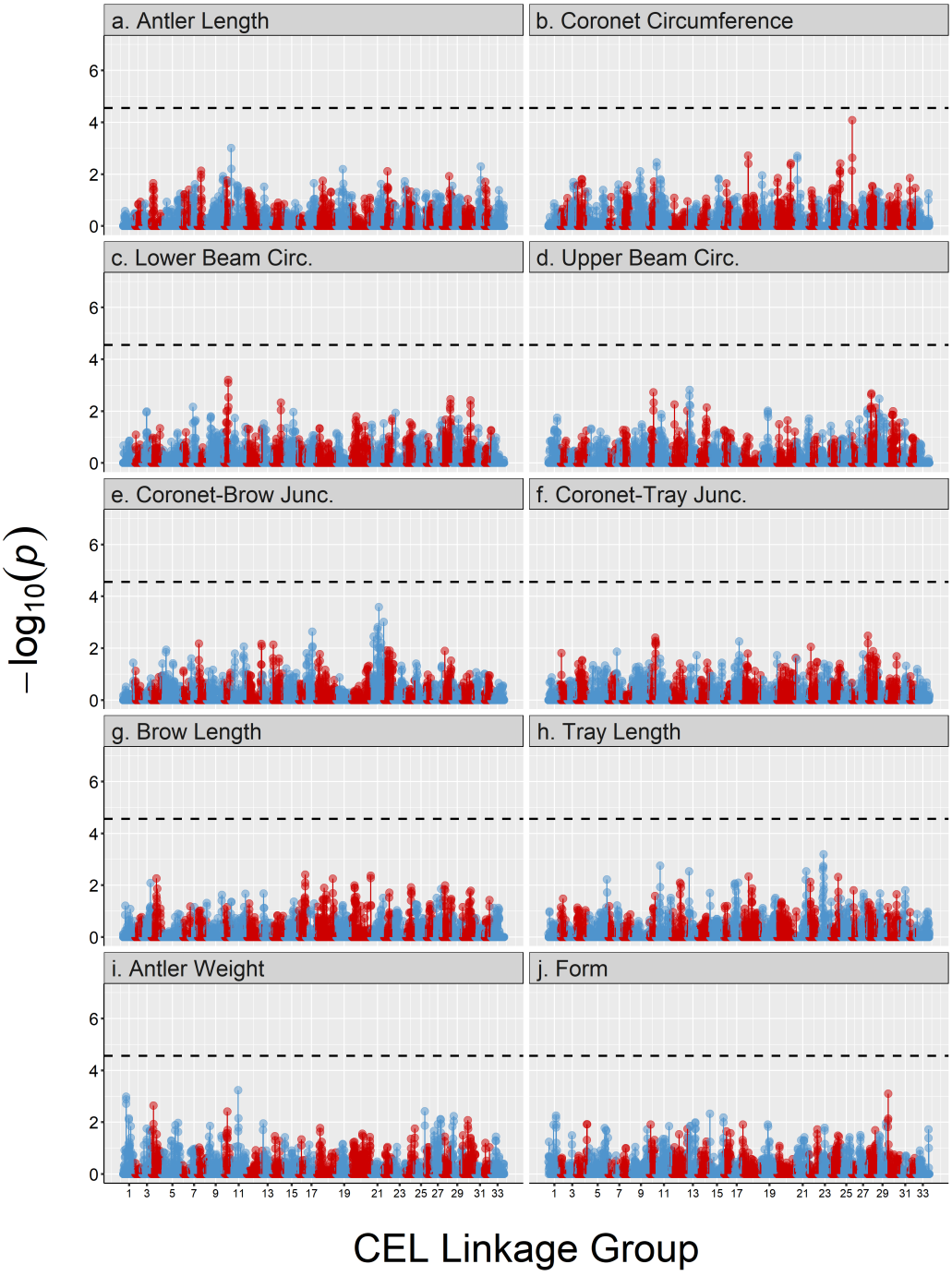

Figure 5: Regional heritability analysis for antler measures. The dashed line indicates the significance threshold equivalent to α = 0.05. Points are colour-coded by chromosome. Underlying data is provided in Table S6

Distribution and quantification of SNP effect sizes

A total of 897 unique SNPs had significant non-zero effects across the ten antler measures (Table 4; full results are provided in Table S11). The number of significant non-zero SNPs ranged from 15 SNPs (antler length) to 279 SNPs (lower beam circumference; Table 4), although antler weight and upper beam circumference had no significant non-zero effect SNPs. Several SNPs showed pleiotropic effects i.e. they were associated with more than one measure (Table S11), with the underlying proportion ranging from 6% (coronet-tray junction) to 68% (tray length). Lower beam circumference and antler form showed distributions that included more extreme SNPs with large effects on phenotype outside the 5% to 95% quantile boundaries, whereas most other measures had more uniformly distributed effect sizes (Table 4). For the 11 antler PCs, only 159 unique SNPs had non-zero effects (Table S10; full results in Table S12). No pleiotropic SNPs were observed, most likely due to the independence of each PC. PC4 and PC9 had no non-zero effect SNP associations. Only about 25% of the 159 SNPs were in common with the 897 SNPs in the antler measure analysis. This was mainly due to the higher order PCs (PC6 to PC11) sharing no SNP associations with any antler measures, while other PCs had similar or more numbers of shared and unique SNPs (PC1 and PC2).

Some of the non-zero effect SNPs with large effect size estimates after FDR explained large proportions of overall genetic and phenotypic variance for their respective traits. The SNP *cela1_red_2_101997097* explained about 17% of the overall additive genetic and 4% of phenotypic variance in antler length (SNP variance = 2.609, SE = 1.094), while for PC8 (which is strongly representative of antler length; Figure 2) the marker *cela1_red_4_41756873* explained 39% of the additive genetic and 4% of the phenotypic variance (SNP variance = 0.019, SE = 0.008). Despite these seemingly large effect marker associations the standard errors for the SNP variance estimates were generally large (see Tables S13 and S14 for summaries of variances, and Tables S15 and S16 for full results for the antler measures and PCs, respectively). Overall, as the uncertainty around the importance of the SNP effects is large and none of these marker achieved genome-wide significance in any of the GWAS, the influence of specific SNP loci on variation in antler measures and PCs must be interpreted with caution.

Table 4: Summary of SNPs with non-zero effects on antler measures. N SNPs is the number of SNPs with non-zero effects. Proportion pleiotropic is the proportion of SNPs with non-zero effects on other antler measures. Maximum and minimum effects are given relative to the data scale (units = cm for lengths, g for weight). Lower and upper quantiles refer to the 5% and 95% boundaries of the effect size distribution respectively.

Antler Measure	**N SNPs**	**Proportion Pleiotropic**	**Maximum Effect**	**Minimum Effect**	**Lower Quantile**	**Upper Quantile**
Antler Length	15	0.4001	0.668	-0.622	-0.619	0.653
Coronet Circ.	56	0.214	0.151	-0.159	-0.152	0.146
Lower Beam Circ.	279	0.136	0.251	-0.151	-0.120	0.144
Upper Beam Circ.	0	-	-	-	-	-
Coronet-Brow Junc.	29	0.138	0.092	-0.084	-0.084	0.091
Coronet-Tray Junc.	110	0.055	0.460	-0.490	-0.435	0.441
Brow Length	272	0.081	0.538	-0.532	-0.484	-0.477
Tray Length	6	0.667	0.357	-0.357	-0.355	0.354
Antler Weight	0	-	-	-	-	-
Form	193	0.124	1.018	-0.097	-0.091	0.096

Discussion

In this study, we have used a genomic approach to determine the genetic architecture of antler morphology in the red deer of Rum. We have shown that antler morphology is heritable and repeatable over an individual's lifetime, and that it is likely to be highly polygenic with a moderate degree of shared genetic architecture across different antler traits. Genome-wide association and regional heritability studies failed to identify any genomic regions associated with antler measures and their principal components, with the exception of a single region on linkage group 21 associated with variation in PC9. Most traits were underpinned by SNPs with uniformly small effect sizes, whereas others, such as coronet circumference and antler form, showed distributions that included some SNPs with larger effects on phenotype. Our findings suggest that antler morphology has a highly polygenic architecture with many loci of small effect. Here, we discuss how our findings build on previous quantitative genetic studies in the Rum red deer system, and how they inform the broader question of the distribution of genetic architectures of sexually selected male weaponry and the consequences for its evolution.

Heritability and repeatability of antler morphology.

All 10 antler measures were significantly heritable (ranging from 0.229 to 0.414, Table 2) and were similar to previous heritability estimates for antler weight and form in the same population (Kruuk *et al.*, 2014). The strong agreement of estimates from both the pedigree and GRM approaches indicate that the SNPs present on the red deer SNP chip are in sufficiently high LD with causative loci to allow accurate estimation of trait heritabilities in this population (Yang *et al.* 2010; Figure 3). Indeed, LD is maintained at a relatively constant level over a distance of up to 1Mb, after which it starts to slowly decay (Figure S1). All antler traits were also highly repeatable, with between 38.5% and 66.1% of the phenotypic variance explained by additive genetic, permanent environment and birth year effects. This indicates that antler morphology is temporally stable over an individual's adult life, despite the annual shedding and regrowth of antlers. Similar findings were found for

the 11 principal components, with lower order PCs generally exhibiting higher heritabilities and repeatabilities (Table S2); we discuss why we think this is the case in the section on genetic correlations and constraints below. It should be noted that the heritabilities may be slightly over-estimated due to any common environments on a fine spatio-temporal scale that cannot captured by the animal models (Stopher *et al.*, 2012). These findings support previous work showing that traits under sexual selection can have substantial underlying genetic variation in wild populations (Kruuk *et al.*, 2008; Merila *et al.*, 2001; Pomiankowski & Moller, 1995), where morphological traits often show heritabilities of a similar magnitude even when associated with fitness (Johnston *et al.*, 2013; Bérénos *et al.*, 2014; Bourret *et al.*, 2017; Malenfant *et al.*, 2018).

The polygenic architecture of antler morphology.

Genome-wide association studies and regional heritability analyses across all antler traits and PCs showed no significant associations, with the exception PC9 (discussed in the next section). Generally, GWAS can only detect loci with moderate to large effects on phenotype and which only partially explain the trait heritabilities, with the remainder termed the “missing heritability” (Manolio *et al.*, 2009; Golan *et al.*, 2014). For example, a meta-analysis of human GWAS found that the heritability attributed to all common SNP variants was significantly higher than that of the SNPs that achieved genome-wide significance. (Shi *et al.*, 2016), meaning that large numbers of “non-significant” SNPs will contribute to the additive genetic variation. To characterise the genetic architecture beyond GWAS alone, we employed two additional approaches. The first, regional heritability (Nagamine *et al.*, 2012), incorporated the haplotypic diversity within genomic regions. This approach detected a large contribution of defined genomic regions to a single PC, but not to any of the other antler measures or PCs. The second, the Empirical Bayes false discovery rate and effect size estimation, incorporated information from the GWAS effect size estimates and their error to show that a substantial number of SNPs had non-zero effects on antler morphology (Stephens, 2016). Taken together, these analyses provide compelling evidence that most aspects of antler morphology have a highly polygenic architecture (Fisher, 1930; Barton *et al.*, 2017). This in line with findings

455 from other studies of wild organisms that have identified polygenic architectures for
456 morphological and life history traits (Robinson *et al.*, 2013; Santure *et al.*, 2013; Pallares
457 *et al.*, 2014; Berenos *et al.*, 2015; Husby *et al.*, 2015). In this study, we modelled antler
458 morphology using both independent measures of antler morphology and a principal
459 component framework to characterise different dimensions of shape variation. An
460 advantage of using both approaches was that it allowed us to identify a greater number of
461 potentially causal loci, which supports the usefulness of this approach when trying to
462 characterise the genetic architecture of a complex morphological trait (such as in Pallares
463 *et al.* 2014).

464 **Genomic regions associated with antler morphology.**

465 Three genomic windows within the CEL linkage group were associated with PC9 at the
466 genome-wide level. The main contributing antler measure to PC9 is coronet circumference
467 The region covered by the most highly associated window explained ∼66% of the additive
468 genetic variance, representing a large part of the overall heritability estimated using the
469 whole GRM (∼19%). The region contains a number of candidate genes among which are
470 gasdermin C (*GSDMC*); MYC proto-oncogene (*MYC*); ArfGAP with SH3 domain, ankyrin
471 repeat and PH domain 1 (*ASAP1*) and cellular communication network factor 4 (*CCN4*).
472 Whilst none have previously been implicated in antler morphology, they have associated
473 functions that make them potential candidate genes. Both the enhancer protein *ASAP1* and
474 *CCN4*, which is a type of connective tissue growth factor, are linked to bone ossification
475 and bone cell differentiation in mice (The Jackson Laboratory, 2019; Schreiber *et al.*, 2019;
476 Maeda *et al.*, 2015), processes which are likely to be vital to antler regeneration, rapid
477 growth and the ability of antlers to withstand impact (Goss, 1983). Upregulation of *GSDMC*
478 is implicated in carcinogenesis in mice, as a consequence of an interrupted growth factor
479 signalling pathway (Miguchi *et al.*, 2016) and *MYC* is a potent oncogene that is implicated
480 in many human cancers and promotes rapid tumor cell proliferation (Beroukhim *et al.*, 2010;
481 Lin *et al.*, 2012); recent work suggests that rapid regeneration of bony antlers has evolved
482 by upregulating cell proliferation pathways while suppressing tumorigenesis (Wang *et al.*,
483 2019).

Despite being linked to compelling candidate gene regions, with our current data it is virtually impossible to determine exactly which genes in this region drive the association with PC9. Furthermore, as PC9 only represents ∼4% of the overall phenotypic variance among all antler PCs, we expect effect sizes of causal loci to be very small. Validating the findings for this association would be challenging, as replication of a similar PC in other deer populations would have to consider its main contributing antler measures (e.g. coronet circumference); additionally, the same variants may not be associated with this trait in different populations. A more feasible approach may be to type a higher density of SNP loci to characterise more variation at (or in tight linkage) with potential causal loci in the Rum deer population.

Genetic correlations and constraints on antler morphology.

Almost all antler traits were positively genetically correlated, with the exception of the coronet-tray junction, which was negatively genetically correlated with tray length, lower beam circumference and antler form. These findings were reflected by the PC analysis, where the PC explaining the most variance in antler morphology (PC1, ∼41%) combined equal information from all antler measures, whereas those explaining declining amounts of variation represented one or two antler traits. The Empirical Bayes analysis identified varying degrees of marker pleiotropy associated with the antler measures (Table 4) that were consistent with the observed genetic correlations. Nevertheless, there were some exceptions, such as for brow length and antler weight, which both showed strong positive genetic correlations yet had small proportions of shared loci (brow length) or no associated loci at all (antler length). This incongruity may be explained by the large variation in the number of non-zero effect SNPs detected between antler measures, which could be due to differences in the effect size distribution of markers.

The large heritabilities of individual antler traits suggest there is potential for response to selection, but our results further add to previous findings that constraints at the genetic level may affect how the population may respond to selection. Previous work showed that a large part of genetic variance in antler weight is not available to selection due to the lack

of genetic covariance between weight and fitness (Kruuk *et al.*, 2002, 2014). In the current study, antler weight was highly correlated with most other antler measures on a genetic level, which may likely indicate that large parts of the genetic variance of these antler measures are also unavailable for selection, thus limiting the evolutionary potential of antler morphology despite large heritability estimates. In the PC analysis, higher order PCs explained much smaller amounts of variation and had very low additive genetic variation. It is possible that these PCs could represent morphologically stable aspects of the antlers, where lower heritabilities could indicate past strong stabilising selection on the combination of trait aspects represented by that PC. Other studies exploring multivariate sexual selection on a suite of traits found that despite large genetic variance in univariate analyses, there can be very little genetic variance available in the trait composition that is the target of selection (Hunt *et al.*, 2007; Van Homrigh *et al.*, 2007).

The discovery that the genetic architecture of antler morphology is highly polygenic also suggests that further evolutionary mechanisms may be partially responsible for the maintenance of genetic variation in this trait. As discussed in the introduction, traits with many genes of small effect can present a large mutational target for the introduction of novel genetic variation which can contribute to the genetic variation in a trait (Rowe & Houle, 1996). Consequently, although selection on polygenic traits can lead to rapid changes in trait mean, under the infinitessimal model the distribution of underlying genetic effects is expected to remain relatively constant, counteracting the loss of genetic variation. (Barton *et al.*, 2017; Sella & Barton, 2019). Finally, pleiotropic effects of loci that share a similar complex architecture with other traits and/or are in LD with loci associated with fitness could maintain genetic variation through conflicts and trade-offs (Lande, 1982).

Conclusions

In this study, we have shown that antler morphology is heritable, has a polygenic genetic architecture, and some degree of shared genetic architecture between different antler measures. A single region association is linked to candidate genes that could potentially

have an effect on antler morphology, but more work would be required to validate this finding in this and other populations. Future work in this system will integrate knowledge of the genomic architecture of antler morphology with fitness measures to further dissect constraints on trait evolution within this population. Ultimately, our findings corroborate the expectation for a quantitative trait such as multidimensional weaponry traits to conform to a polygenic genetic architecture of many genes with small effects.

Author Contributions

L.P. and S.E.J. designed the study. J.M.P and L.K provided the data. L.P., J.H and S.E.J. analysed the data. L.P. and S.E.J. wrote the first draft of the paper and all authors contributed to revisions.

Acknowledgements

We thank Alison Morris, Sean Morris, Martin Baker, Fiona Guinness, Tim Clutton-Brock and many others for collecting field data and DNA samples over the course of the long-term study. We thank Scottish Natural Heritage for permission to work on the Isle of Rum National Nature Reserve. Andy Arthur kindly provided Figure 1. Philip Ellis prepared samples for DNA extraction and the Wellcome Trust Clinical Research Facility Genetics Core in Edinburgh performed the genotyping. This work made extensive use of the University of Edinburgh Compute and Data Facility (http://www.ecdf.ed.ac.uk/). The long-term project on Rum red deer is funded by the UK Natural Environment Research Council (NERC) and the SNP genotyping was funded by a European Research Council Advanced Grant to J.M.P.. L.P is supported by a NERC E3 Doctoral Training Programme PhD Studentship. S.E.J. is supported by a Royal Society University Research Fellowship.

References

Andersson M (1994) *Sexual selection*. Princeton University Press, Princeton, NJ, USA.

Aulchenko YS, Ripke S, Isaacs A, Van Duijn CM (2007) GenABEL: an R library for genome-wide association analysis. *Bioinformatics*, **23**, 1294–1296.

Barson NJ, Aykanat T, Hindar K, *et al.* (2015) Sex-dependent dominance at a single locus maintains variation in age at maturity in salmon. *Nature*, **528**, 405–408.

Barton N, Etheridge A, Véber A (2017) The infinitesimal model: Definition, derivation, and implications. *Theoretical Population Biology*, **118**, 50–73.

Berenos C, Ellis PA, Pilkington JG, Lee SH, Gratten J, Pemberton JM (2015) Heterogeneity of genetic architecture of body size traits in a free-living population. *Molecular Ecology*, **24**, 1810–1830.

Bérénos C, Ellis PA, Pilkington JG, Pemberton JM (2014) Estimating quantitative genetic parameters in wild populations: A comparison of pedigree and genomic approaches. *Molecular Ecology*, **23**, 3434–3451.

Beroukhim R, Mermel CH, Porter D, *et al.* (2010) The landscape of somatic copy-number alteration across human cancers. *Nature*, **463**, 899–905.

Bourret A, Belisle M, Pelletier F, Garant D (2017) Evolutionary potential of morphological traits across different life-history stages. *Journal of Evolutionary Biology*, **30**, 616–626.

Brauning R, Fisher PJ, McCulloch AF, *et al.* (2015) Utilization of high throughput genome sequencing technology for large scale single nucleotide polymorphism discovery in red deer and Canadian elk. *bioRxiv*.

Butler DG, Cullis BR, Gilmour AR, Gogel BJ (2009) Mixed Models for S language Environments: ASReml-R reference manual.

Chang CC, Chow CC, Tellier LC, Vattikuti S, Purcell SM, Lee JJ (2015) Second-generation PLINK: Rising to the challenge of larger and richer datasets. *GigaScience*, **4**, 7.

587 Charmantier A, Gienapp P (2014) Climate change and timing of avian breeding and
588 migration: evolutionary versus plastic changes. *Evolutionary Applications*, **7**, 15–28.

589 Chenoweth SF, McGuigan K (2010) The Genetic Basis of Sexually Selected Variation.
590 *Annual Review of Ecology, Evolution, and Systematics, Vol 41*, **41**, 81–101.

591 Clutton-Brock T, Guiness F, Albon S (1982) *Red Deer. Behaviour and Ecology of Two*
592 *Sexes*. University of Chicago Press.

593 Connallon T, Hall MD (2018) Genetic constraints on adaptation: a theoretical primer for the
594 genomics era. *Annals of the New York Academy of Sciences*, **1422**, 65–87.

595 Davis EB, Brakora KA, Lee AH (2011) Evolution of ruminant headgear: A review.
596 *Proceedings of the Royal Society B: Biological Sciences*, **278**, 2857–2865.

597 Devlin B, Roeder K (1999) Genomic control for association studies. *Biometrics*, **55**, 997–
598 1004.

599 Dobzhansky T (1971) *Genetics of the evolutionary process*, vol. 139. Columbia University
600 Press.

601 Dugand RJ, Tomkins JL, Kennington WJ (2019) Molecular evidence supports a genic
602 capture resolution of the lek paradox. *Nature Communications*, **10**, 1359.

603 Emlen DJ (1994) E nvironm ental control of horn length dim orphism in the beetle
604 Onthophagus acuminatus (C oleoptera: Scarabaeidae). Tech. Rep..

605 Falconer DS, Mackay TFC (1996) *Introduction to quantitative genetics*. Longman, Harlow,
606 fourth edi edn..

607 Fisher RA (1930) *The genetical theory of natural selection*. The Clarendon Press, Oxford.

608 Golan D, Lander ES, Rosset S (2014) Measuring missing heritability: inferring the
609 contribution of common variants. *Proceedings of the National Academy of Sciences*
610 *of the United States of America*, **111**, 5272–81.

611 Goss RJ (1983) *Deer Antlers: Regeneration, Function and Evolution*. Academic Press.

612 Griffith SC, Owens IP, Burke T (1999) Environmental determination of a sexually selected
613 trait. *Nature*, **400**, 358–360.

614 Henderson CR (1975) Best Linear Unbiased Estimation and Prediction under a Selection
615 Model. *Biometrics*, **31**, 423–447.

616 Hendrickx F, De Corte Z, Sonet G, Belleghem SMV, Köstlbacher S, Vangestel C (2021) A
617 masculinizing supergene underlies an exaggerated male reproductive morph in a spider.
618 *bioRxiv*, p. 2021.02.09.430505.

619 Huisman J (2017) Pedigree reconstruction from SNP data: parentage assignment, sibship
620 clustering and beyond. *Molecular Ecology Resources*, **17**, 1009–1024.

621 Huisman J, Kruuk LEB, Ellis PA, Clutton-Brock T, Pemberton JM (2016) Inbreeding
622 depression across the lifespan in a wild mammal population. *Proceedings of the National*
623 *Academy of Sciences of the United States of America*, **113**, 3585–3590.

624 Hunt J, Blows MW, Zajitschek F, Jennions MD, Brooks R (2007) Reconciling strong
625 stabilizing selection with the maintenance of genetic variation in a natural population
626 of black field crickets (Teleogryllus commodus). *Genetics*, **177**, 875–880.

627 Husby A, Kawakami T, Rönnegård L, Smeds L, Ellegren H, Qvarnström A (2015) Genome-
628 wide association mapping in a wild avian population identifies a link between genetic and
629 phenotypic variation in a life-history trait. *Proceedings of the Royal Society B: Biological*
630 *Sciences*, **282**.

631 Jackson CH (2011) Multi-State Models for Panel Data: The msm Package for
632 R. *Journal of Statistical Software*, **38**, 1–28.

633 Jamieson A, Anderson SJ, Fuller J, Côté SD, Northrup JM, Shafer AB (2020) Heritability
634 estimates of antler and body traits in white-tailed deer (odocoileus virginianus) from
635 genomic-relatedness matrices. *Journal of Heredity*, **111**, 429–435.

636 Johnston SE, Gratten J, Berenos C, *et al.* (2013) Life history trade-offs at a single locus
637 maintain sexually selected genetic variation. *Nature*, **502**, 93–95.

638 Johnston SE, Huisman J, Ellis PA, Pemberton JM (2017) A High-Density Linkage Map
639 Reveals Sexual Dimorphism in Recombination Landscapes in Red Deer (Cervus
640 elaphus). *G3-Genes Genomes Genetics*, **7**, 2859–2870.

641 Johnston SE, Huisman J, Pemberton JM (2018) A Genomic Region Containing REC8
642 and RNF212B Is Associated with Individual Recombination Rate Variation in a Wild
643 Population of Red Deer (Cervus elaphus). *G3: Genes|Genomes|Genetics*, **8**, 2265–
644 2276.

645 Johnston SE, McEwan JC, Pickering NK, *et al.* (2011) Genome-wide association mapping
646 identifies the genetic basis of discrete and quantitative variation in sexual weaponry in a
647 wild sheep population. *Molecular Ecology*, **20**, 2555–2566.

648 Kingsolver JG, Hoekstra HE, Hoekstra JM, *et al.* (2001) The strength of phenotypic
649 selection in natural populations. *American Naturalist*, **157**, 245–261.

650 Kotiaho JS, Simmons LW, Tomkins JL (2001) Towards a resolution of the lek paradox.
651 *Nature*, **410**, 684–686.

652 Kruuk LEB, Clutton-Brock T, Pemberton JM (2014) Case study: quantitative genetics
653 and sexual selection of weaponry in a wild ungulate. In *Quantitative genetics in the*
654 *wild* (edited by A Charmantier, D Garant, LEB Kruuk), chap. 10, pp. 160–176. Oxford
655 University Press, 1st edn..

656 Kruuk LEB, Slate J, Pemberton JM, Brotherstone S, Clutton-Brock TH (2002) Antler size
657 in red deer: hertability and selection but no evolution. *Evolution*, **56**, 1683–1695.

658 Kruuk LEB, Slate J, Wilson AJ (2008) New Answers for Old Questions: The Evolutionary
659 Quantitative Genetics of Wild Animal Populations. *Annual Review of Ecology Evolution*
660 *and Systematics*, **39**, 525–548.

661 Kuijper B, Pen I, Weissing FJ (2012) A guide to sexual selection theory. *Annual Review of*
662 *Ecology, Evolution, and Systematics*, **43**, 287–311.

663 Lande R (1982) A Quantitative Genetic Theory of Life History Evolution. *Ecology*, **63**,
664 607–615.

665 Lande R, Arnold SJ (1983) The Measurement of Selection on Correlated Characters.
666 *Evolution*, **37**, 1210–1226.

667 Lewontin RC, *et al.* (1974) *The genetic basis of evolutionary change*, vol. 560. Columbia
668 University Press New York.

669 Lin CY, Lovén J, Rahl PB, *et al.* (2012) Transcriptional amplification in tumor cells with
670 elevated c-Myc. *Cell*, **151**, 56–67.

671 Lorch PD, Proulx S, Rowe L, Day T (2003) Condition-dependent sexual selection can
672 accelerate adaptation. *Evolutionary Ecology Research*, **5**, 867–881.

673 Lukefahr SD, Jacobson HA (1998) Variance Component Analysis and Heritability of Antler
674 Traits in White-Tailed Deer. *The Journal of Wildlife Management*, **62**, 262.

675 Maeda A, Ono M, Holmbeck K, *et al.* (2015) WNT1-Induced Secreted Protein-1 (WISP1),
676 a novel regulator of bone turnover and Wnt signaling. *Journal of Biological Chemistry*,
677 **290**, 14004–14018.

678 Malenfant RM, Davis CS, Richardson ES, Lunn NJ, Coltman DW (2018) Heritability of
679 body size in the polar bears of Western Hudson Bay. *Molecular Ecology Resources*, **18**,
680 854–866.

681 Malo AF, Roldan ERS, Garde J, Soler AJ, Gomendio M (2005) Antlers honestly advertise
682 sperm production and quality. *Proceedings of the Royal Society of London B: Biological*
683 *Sciences*, **272**, 149–57.

684 Manolio TA, Collins FS, Cox NJ, *et al.* (2009) Finding the missing heritability of complex
685 diseases. *Nature*, **461**, 747–753.

686 Martínez-Ruiz C, Knell RJ (2017) Sexual selection can both increase and decrease
687 extinction probability: reconciling demographic and evolutionary factors. *Journal of*
688 *Animal Ecology*, **86**, 117–127.

689 McNamara JM, Houston AI (2009) Integrating function and mechanism. *Trends in Ecology*
690 *& Evolution*, **24**, 670–675.

691 Merila J, Sheldon BC, Kruuk LEB, Merilä J, Sheldon BC, Kruuk LEB (2001) Explaining
692 stasis: microevolutionary studies in natural populations. *Genetica*, **112**, 199–222.

693 Miguchi M, Hinoi T, Shimomura M, *et al.* (2016) Gasdermin C is upregulated by inactivation
694 of transforming growth factor β receptor type II in the presence of mutated Apc,
695 promoting colorectal cancer proliferation. *PLoS ONE*, **11**.

696 Nagamine Y, Pong-Wong R, Navarro P, *et al.* (2012) Localising Loci underlying Complex
697 Trait Variation Using Regional Genomic Relationship Mapping. *Plos One*, **7**.

698 Nussey DH, Kruuk LE, Morris A, Clements MN, Pemberton JM, Clutton-Brock TH (2009)
699 Inter- And intrasexual variation in aging patterns across reproductive traits in a wild red
700 deer population. *American Naturalist*, **174**, 342–357.

701 Oba S, Sato M, Takemasa I, Monden M, Matsubara K, Ishii S (2003) A Bayesian missing
702 value estimation method for gene expression profile data. *Bioinformatics*, **19**, 2088–
703 2096.

704 Pallares LF, Harr B, Turner LM, Tautz D (2014) Use of a natural hybrid zone for genomewide
705 association mapping of craniofacial traits in the house mouse. *Molecular Ecology*, **23**,
706 5756–5770.

707 Pomiankowski A, Moller AP (1995) A Resolution of the Lek Paradox. *Proceedings of the*
708 *Royal Society B-Biological Sciences*, **260**, 21–29.

709 Ritchie MG (2007) Sexual selection and speciation. *Annu. Rev. Ecol. Evol. Syst.*, **38**, 79–
710 102.

711 Robinson MR, Pilkington JG, Clutton-brock TH, Pemberton JM, Kruuk LEB (2006) Live fast,
712 die young: trade-offs between fitness components and sexually antagonistic selection on
713 weaponry in Soay sheep. *Evolution*, **60**, 2168–2181.

714 Robinson MR, Santure AW, DeCauwer I, Sheldon BC, Slate J (2013) Partitioning of
715 genetic variation across the genome using multimarker methods in a wild bird population.
716 *Molecular Ecology*, **22**, 3963–3980.

717 Rönnegård L, McFarlane SE, Husby A, Kawakami T, Ellegren H, Qvarnstrom A (2016)
718 Increasing the power of genome wide association studies in natural populations using
719 repeated measures - evaluation and implementation. *Methods in Ecology and Evolution*,
720 **7**, 792–799.

721 Rowe L, Houle D (1996) The lek paradox and the capture of genetic variance by condition
722 dependent traits. *Proceedings of the Royal Society B-Biological Sciences*, **263**, 1415–
723 1421.

724 Ruzicka F, Hill MS, Pennell TM, *et al.* (2019) Genome-wide sexually antagonistic variants
725 reveal long-standing constraints on sexual dimorphism in fruit flies. *PLOS Biology*, **17**,
726 e3000244.

727 Santure AW, De Cauwer I, Robinson MR, Poissant J, Sheldon BC, Slate J (2013) Genomic
728 dissection of variation in clutch size and egg mass in a wild great tit (Parus major
729) population. *Molecular Ecology*, **22**, 3949–3962.

730 Santure AW, Garant D (2018) Wild GWAS-association mapping in natural populations.
731 *Molecular Ecology Resources*, **18**, 729–738.

732 Schreiber C, Saraswati S, Harkins S, *et al.* (2019) Loss of ASAP1 in mice impairs
733 adipogenic and osteogenic differentiation of mesenchymal progenitor cells through
734 dysregulation of FAK/ Src and AKT signaling. *PLoS Genetics*, **15**, e1008216.

735 Sella G, Barton NH (2019) Thinking about the Evolution of Complex Traits in the Era of
736 Genome-Wide Association Studies. *Annual Review of Genomics and Human Genetics*,
737 **20**, 461–493.

738 Servedio MR, Bürger R (2014) The counterintuitive role of sexual selection in species
739 maintenance and speciation. *Proceedings of the National Academy of Sciences*, **111**,
740 8113–8118.

741 Shi H, Kichaev G, Pasaniuc B (2016) Contrasting the Genetic Architecture of 30 Complex
742 Traits from Summary Association Data. *The American Journal of Human Genetics*, **99**,
743 139–153.

744 Stacklies W, Redestig H (2018) Imputing missing values using the pcaMethods package.

745 Stephens M (2016) False discovery rates: a new deal. *Biostatistics*, **18**, kxw041.

746 Stopher KV, Walling CA, Morris A, *et al.* (2012) Shared Spatial Effects on Quantitative
747 Genetic Parameters: Accounting for Spatial Autocorrelation and Home Range Overlap
748 Reduces Estimates of Heritability in Wild Red Deer. *Evolution*, **66**, 2411–2426.

749 Svensson EI, Gosden TP (2007) Contemporary evolution of secondary sexual traits in the
750 wild. *Functional Ecology*, **21**, 422–433.

The Jackson Laboratory (2019) Mouse Genome Database (MGD) at the Mouse Genome Informatics website.

Timpson NJ, Greenwood CMT, Soranzo N, Lawson DJ, Richards JB (2018) Genetic architecture: the shape of the genetic contribution to human traits and disease. *Nature Reviews Genetics*, **19**, 110–124.

Van Den Berg GH, Garrick DJ (1997) Inheritance of adult velvet antler weights and live weights in farmed red deer. *Livestock Production Science*, **49**, 287–295.

Van Homrigh A, Higgie M, McGuigan K, Blows MW (2007) The depletion of genetic variance by sexual selection. *Current Biology*, **17**, 528–532.

Wang Y, Zhang C, Wang N, *et al.* (2019) Genetic basis of ruminant headgear and rapid antler regeneration. *Science (New York, N.Y.)*, **364**, eaav6335.

Wang Z, Yang RC, Goonewardene LA, Huedepoh C (1999) Genetic analysis of velvet antler yield in farmed elk (Cervus elaphus). *Canadian Journal of Animal Science*, **79**, 569–571.

Wilkinson GS, Breden F, Mank JE, *et al.* (2015) The locus of sexual selection: moving sexual selection studies into the post-genomics era. *Journal of Evolutionary Biology*, **28**, 739–755.

Williams JD, Krueger WF, Harmel DH (1994) Heritabilities for antler characteristics and body weight in yearling white-tailed deer. *Heredity*, **73**, 78–83.

Yang J, Benyamin B, McEvoy BP, *et al.* (2010) Common SNPs explain a large proportion of the heritability for human height. *Nature Genetics*, **42**, 565–569.

Yang J, Lee H, Goddard ME, Visscher PM (2011a) GCTA: A Tool for Genome-wide Complex Trait Analysis. *The American Journal of Human Genetics*, **88**, 76–82.

Yang J, Manolio TA, Pasquale LR, *et al.* (2011b) Genome partitioning of genetic variation for complex traits using common SNPs. *Nature Genetics*, **43**, 519–U44.

Yengo L, Sidorenko J, Kemper KE, *et al.* (2018) Meta-analysis of genome-wide association studies for height and body mass index in $\sim$700000 individuals of European ancestry. *Human molecular genetics*, **27**, 3641–3649.